Scaling Analysis and Distribution of the Rotational Correlation Times of a Tracer in Rubbery and Glassy Poly(vinyl acetate): An Electron Spin Resonance Investigation

M. Faetti, M. Giordano, D. Leporini,* and L. Pardi

Dipartimento di Fisica, Universita' di Pisa, Piazza Torricelli 2, I-56100 Pisa, Italy, and Istituto Nazionale di Fisica della Materia, UdR Pisa, Piazza Torricelli 2, I-56100 Pisa, Italy

Received July 28, 1998; Revised Manuscript Received December 15, 1998

ABSTRACT: We studied by ESR the rotational motion of a paramagnetic tracer (a deuterated ^{15}N-enriched nitroxide) in poly(vinyl acetate) (PVAc). The reorientation of the tracer occurs via jumps of about 50° with a heterogeneous distribution of correlation times. Depending on the temperature range, the average correlation time $\langle\tau\rangle$ scales as the α, β, and γ relaxation times of PVAc, i.e., $\langle\tau\rangle = C_i\langle\tau\rangle_i$, $i = \alpha, \beta, \gamma$. On cooling, $\langle\tau\rangle$ tracks the α relaxation to about the $\alpha-\beta$ bifurcation temperature and then the β relaxation down to the glass transition. In glassy PVAc $\langle\tau\rangle/\langle\tau\rangle_\gamma = C_\gamma \approx 1$.

I. Introduction

The time scales of the dynamic processes taking place in polymers span a wide range which must be unavoidably studied by different spectroscopic or relaxation techniques. The information is often provided in terms of the correlation time of scalar (e.g., density), vector (e.g., dipoles), or tensor (e.g., susceptibility) quantities. The comparison of the different correlation times is not trivial since they usually refer to quantities monitoring different aspects of the polymer chain dynamics. On the other hand, a consistent picture of the polymer dynamics by integrating the results coming from different techniques is highly desirable. The matter becomes particularly delicate when the information is drawn by suitable tracers dissolved in the polymeric host. In this case, even if the coupling between the tracer relaxation and the free volume is anticipated, the amount of information gained on the relaxation properties of the polymer is less obvious.

In a series of papers Dhinojwala et al.,[1−4] Hooker and Torkelson,[5] and Blackburn et al.[6] demonstrated that the reorientation of *large* tracers with nanometer size is well coupled to the α-relaxation of polymers. Remarkably, for the smaller scale motions involving internal rotations and/or isomerizations of the tracer, significant decoupling from the α-relaxation has been evidenced by Hooker and Torkelson[5] and Ye et al.[7] via time-resolved fluorescence measurements. In particular, Ye et al. demonstrated that the internal rotations of cromophores exhibit a well-defined change of dynamic regime at about 30−50 K above the glass transition temperature T_g.[7] Similar decoupling phenomena in the reorientation of paramagnetic tracers were observed by the present authors in low-molecular-weight glass-formers[8−11] and polymers.[12,13]

The above studies suggest that tracers with subnanometer size may be effectively coupled to local relaxations, e.g., β, γ relaxations. Being motivated by these remarks, we investigated in great detail the rotational relaxation of a paramagnetic tracer with subnanometer size in poly(vinyl acetate) (PVAc) by electron spin resonance spectroscopy (ESR).

Electron spin resonance spectroscopy (ESR) is of current use to study the rotational dynamics of radicals, so-called "spin probes", dissolved as tracers in liquid hosts,[14,15] polymeric materials,[16−18] and polymeric liquid crystals.[19,20] Alternatively, the tracers may be also chemically attached to the host molecules as "spin-labels".[21−23] The radicals of current use are nitroxides[14,15] whose ESR line shape is rich in details that must be analyzed by proper numerical programs in order to gain full information on the finer details of the tracer reorientation.[25,26] In this work a fully deuterated ^{15}N-enriched nitroxide spin probe is used. Differently from the customary ^{14}N nitroxides, the ^{15}N deuterated nitroxides exhibit an ESR line shape with a simplified pattern and a smaller residual inhomogeneous broadening.

The study, which is carried out on a wide temperature range (200−450 K), collects convincing evidence on the correlation between the reorientation of the tracer and the α, β, γ relaxation modes of PVAc.[27] It is found that, at temperatures higher than the one where the α and the β processes bifurcate, $T_{\alpha-\beta}$,[27] the average rotational correlation time of the tracer $\langle\tau\rangle$ is proportional to the α relaxation time of PVAc, $\langle\tau\rangle_\alpha$. In the range $T_{\alpha-\beta} > T > T_g$ (T_g is the PVAc glass transition temperature) $\langle\tau\rangle$ is proportional to the β relaxation time $\langle\tau\rangle_\beta$, whereas $\langle\tau\rangle$ is comparable to the γ relaxation time below T_g. These findings are summarized by the scaling relation

$$\langle\tau\rangle = C_i\langle\tau\rangle_i,\ i = \alpha, \beta, \gamma \qquad (1)$$

It is understood that the choice of the i index depends on the temperaure. The existence of a correlation between the dielectric modes and the reorientation of the tracer is also supported by the observation that the tracer, which reorientates by jumps of about 50°, exhibits a heterogeneous distribution of correlation times whose breadth is close to the one of the dielectric relaxation times.

II. Experimental Section

A. Samples. The polymer under study is poly(vinyl acetate) (PVAc) (Figure 1) which was obtained commercially and used

* To whom correspondence should be addressed. e-mail: leporini@mailbox.difi.unipi.it.

10.1021/ma981178x CCC: $18.00
Published on Web 02/24/1999

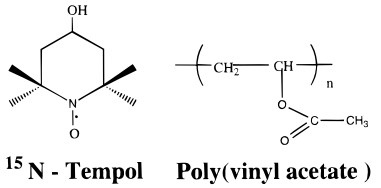

Figure 1. Structures of the ^{15}N-DTEMPOL tracer (left) and PVAc monomer (right).

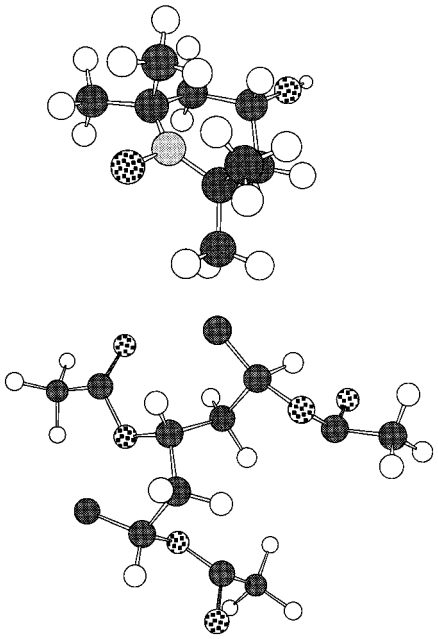

Figure 2. 3D model of the ^{15}N-DTEMPOL tracer (top) and of a PVAc fragment (bottom).

as received. The 3D model of a PVAc fragment is shown in Figure 2. The weight-average molecular weight is $M_w = 197.6$ kg/mol, and the dispersity is 3.67. The calorimetric glass transition temperature is $T_g = 318$ K.

The tracer is the perdeuterated nitroxide 4-(hydroxyl)-2,2,6,6-tetramethyl-piperidine, 1-^{15}N-1 oxyl (^{15}N-DTEMPOL, MSD Isotopes Inc.), which is nearly spherical with a van der Waals volume of about 180 Å (Figure 1). The 3D model of ^{15}N-DTEMPOL is shown in Figure 2. The unpaired electron with spin $S = {}^1/_2$ of the tracer interacts with the ^{15}N nucleus having spin $I = {}^1/_2$. It must be noted that the customary nitroxide radicals have one ^{14}N nucleus ($I = 1$) and are not deuterated. The ESR line shape of the ^{14}N isotope has a more complex pattern, whereas the superhyperfine coupling of the protons with the unpaired spin results in undesirable broadening. The magnetic parameters of the tracer are virtually temperature-independent and were carefully measured by fitting the "powder" ESR line shape, i.e., the line shape measured at very low temperature where the line broadening is not due to the reorientation of the tracer.[19,26] The best fit is shown in Figure 3.

The sample was prepared at Max-Planck Institut für Polymerforschung in Mainz by dissolving the tracer in PVAc according to the solution method.[23,28] The tracer concentration was less than 0.5% in weight. Before starting the ESR measurements, the sample was carefully dried at about 370 K in a vacuum for 36 h and sealed in a standard ESR tube. Tracer aggregation, which should result in a huge broadening of the ESR line shape, was never evidenced.

B. ESR Spectroscopy. The ESR measurements were carried out by using a Bruker spectrometer ER200D equipped with an X-band bridge ($\nu_0 = 10$ GHz), a NMR gaussmeter ER035M, and a gas-flow variable-temperature unit with a temperature stability of about 0.1 K.

The quantity that is detected by the ESR spectroscopy is the magnetization of the spin probes ensemble **M**. More

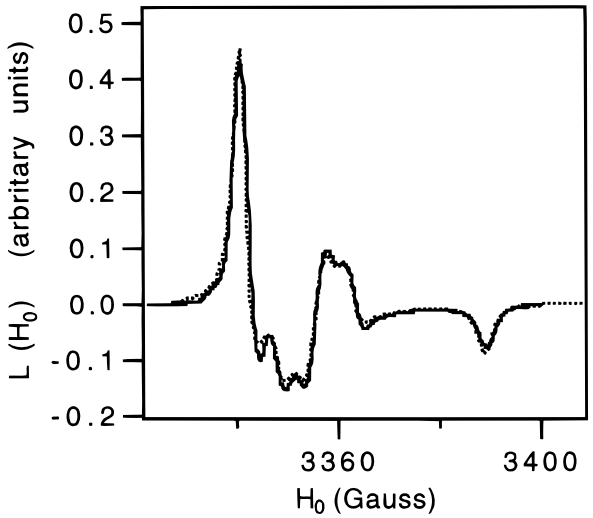

Figure 3. Best fit (dotted line) of the ESR line shape spectrum at 112 K (powder spectrum). The best fit magnetic parameters are $g_{xx} = 2.0095$, $g_{yy} = 2.006$, $g_{zz} = 2.002$; $A_{xx} = 9.3$ (G), $A_{yy} = 9.4$ (G), $A_{zz} = 48.2$ (G); $T_2^{-1} = 1.75$ (G).

precisely, the technique measures the component of **M**, M_x, which is perpendicular to the polarizing static magnetic field H_0 (H_0 defines the Z axis of the laboratory frame). The relaxation of **M** is governed by the radical reorientation. In fact, the relevant magnetic interactions are anisotropic, and their principal axes are fixed in the molecular frame of the tracer. Being the electron spin quantized in the laboratory frame, the reorientation of the spin probe results in random time-dependent magnetic fields relaxing the magnetization **M**.[14,15]

In the ESR X-band spectroscopy a microwave field of frequency ν ($\nu \approx 10$ GHz) induces σ transitions between the Zeeman multiplets created by the magnetic field H_0. Each multiplet of the ^{15}N-DTEMPOL tracer has $(2I + 1) = 2$ hyperfine lines, and then two main transitions are found at $\nu \approx \nu_0$ when H_0 is swept ($\nu_0 = \gamma H_0/2\pi$ is the Larmor frequency, γ being the magnetogyric factor). Being the amplitude of the microwave field small, the spin ensemble responds linearly, and the ESR line shape $L(H_0)$ is expressed in terms of the Laplace transform of the time correlation function of M_X as[14,15]

$$L(H_0) = C\frac{\partial}{\partial H_0}\mathrm{Re}\int_0^\infty \langle M_x M_x(t)\rangle e^{i\gamma H_0 t}\, dt \qquad (2)$$

The brackets mean a proper thermal average, Re{z} is the real part of z, C is a constant, $i^2 = -1$, and the derivative is due to the phase detection of the ESR signal. The theory of the ESR line shape and the details on the numerical expansion of $L(H_0)$ in terms of continued fractions by using suitable memory functions are found elsewhere.[19,25] Here, we recall that the time evolution of M_x is governed by the equation of motion[14,15,19,25]

$$\frac{\partial}{\partial t}M_x(t) = i[H, M_x(t)] + \Gamma M_x(t) \qquad (3)$$

where H is the suitable spin Hamiltonian ($[A, B] = AB - BA$). The rotational dynamics of the spin probe is modeled via the Γ operator. The explicit form of the Γ operator for spherically symmetric molecules rotating by instantaneous random jumps of fixed size ϕ after a mean residence time, τ_0, was derived long time ago.[29] Recent applications to the rotational motion of tracers in supercooled liquids are reported.[30] The model expresses the rotational correlation time (the area below the correlation function of the spherical harmonic $Y_{2,0}$) as

$$\tau = \tau_0/[1 - \sin(5\phi/2)/(5\sin\phi/2)] \qquad (4)$$

In the limit $\phi \ll 1$ the jump model reduces to the isotropic

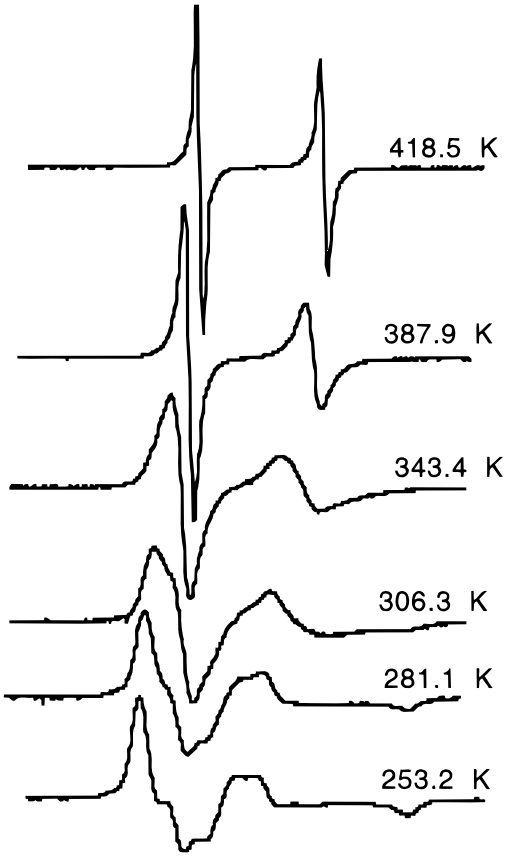

Figure 4. ESR spectra of TEMPOL in PVAc at different temperatures. The strong temperature dependence of the line shape must be noted.

diffusion model and τ becomes

$$\tau = \frac{1}{6D} \equiv \frac{\tau_0}{\phi^2} \tag{5}$$

where D is the rotational diffusion coefficient. The rotational correlation times are drawn by fitting the ESR line shape. The adjustable parameters are τ_0, ϕ, and the magnetic parameters of the tracer. The latter are measured according to the customary procedure detailed in section IIA.

III. Results and Discussion

A. Heterogeneous Jump Reorientation of the Tracer. Figure 4 shows the temperature dependence of the ESR line shape. The strong changes emphasize the sensitivity of the ESR spectroscopy to the rotational dynamics of the tracers. In particular, above 360 K the line shape exhibits the two-line "Redfield" pattern, which is the signature of a spin system with $S = {}^1/_2$ and $I = {}^1/_2$ in the presence of motional narrowing.[14,15,19] Below 360 K, the pattern of the ESR line shape is richer in details and extremely sensitive to the details of the reorientation. In this temperature range the comparison between different models can be carried out quite effectively.[30]

Figure 5a,b shows the comparison carried out at 273 K between the experimental ESR line shape and the predictions of the diffusion ($\phi \ll 1$) and the jump (finite ϕ) models. The jump model improves the agreement with respect to the diffusional one, but discrepancies are still apparent around 3360 G.

It is well-known that polymeric materials exhibit a strong heterogeneous character. Then, the simple assumption of a single correlation time τ for the TEMPOL tracer may be questioned. In fact, previous 2D ELDOR work concerning the rotational dynamics of the present tracer in glassy PVAc at 250 K evidenced a heterogeneous correlation time distribution.[23] Furthermore, dynamic heterogeneities composed of fast and slow relaxators were detected by NMR at $T_g + 10$ K in PVAc.[24] Being motivated by these remarks, we considered the ESR line shape $L(H_0)$ as a weighted superposition of contributions:

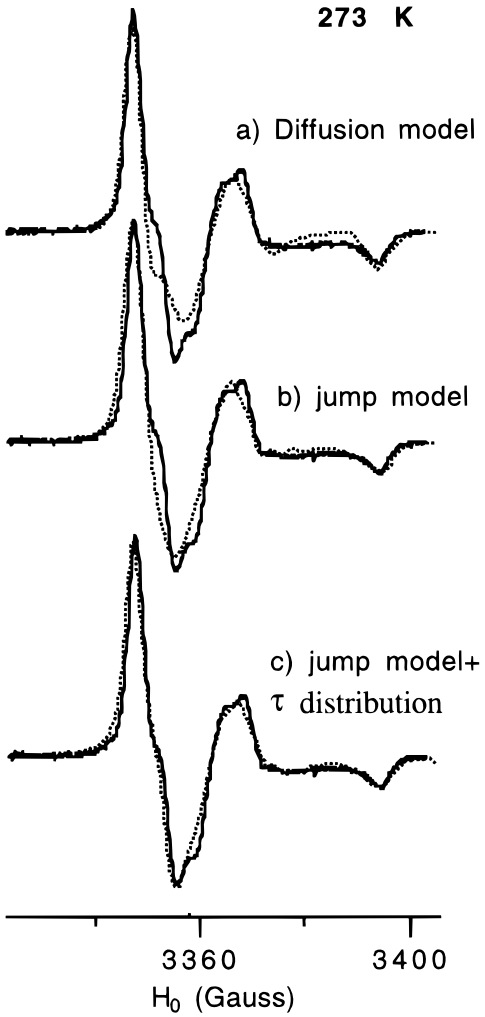

Figure 5. Best fit of the ESR line shape at 273 K (continuous line) by using the diffusion model ($\phi = 0$, $\tau = 2.45 \times 10^{-8}$ s) and the jump model ($\phi = 50°$, $\tau = 2.6 \times 10^{-8}$ s) and by accounting for a heterogeneous correlation time distribution ($\phi = 60°$, $\langle\tau\rangle = 4 \times 10^{-8}$ s, $\sigma = 1.01$).

$$L(H_0) = \int_{-\infty}^{+\infty} \mathrm{d}\ln(\tau)\, \rho(\tau)\, L(H_0,\tau) \tag{6}$$

where $L(H_0,\tau)$ and $\rho(\tau)$ are the ESR line shape of tracer with correlation time τ and the τ distribution, respectively. We identify $\rho(\tau)$ with the log-Gauss distribution

$$\rho(\tau) = \frac{1}{(2\pi\sigma^2)^{1/2}} \exp\left[-\frac{1}{2\sigma^2}\left(\ln\frac{\tau}{\tau^*}\right)^2\right] \tag{7}$$

σ is a width parameter. $\rho(\tau)$ is maximum at τ^* . The log-Gauss distribution follows if the molecular motion occurs via activated jumps over normally distributed energy barriers ΔE. Equation 7 is also derived by picturing the relaxation as a "series" process, so that

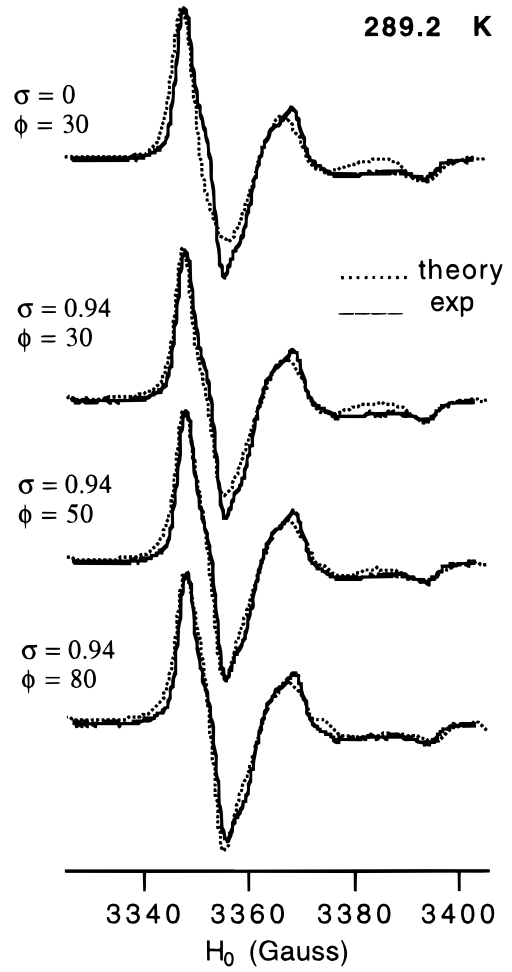

Figure 6. Best fit of the ESR line shape at 289.2 K (continuous line) by using a single correlation time (top, $\tau = 1.62 \times 10^{-8}$ s, $\phi = 30°$) and the log-Gauss distribution with a width $\sigma = 0.94$ and different jump angles. Best results are reached by setting $\phi \approx 50°$.

the relaxing variable (in our case, the tracer orientation) is written as product of independent variables. On this basis the central limit theorem yields the log-Gauss distribution.[31] Use of the log-Gauss distribution in dielectric studies on PVAc is reported.[32] Alternative choices for $\rho(\tau)$ were also considered with no meaningful improvement. In particular, replacing the log-Gauss distribution with a rectangular one on the log τ scale did not yield any meaningful change in the quality of the fit.

To investigate the effect of the time distribution on the ESR spectra, we have fitted the experimental results with eq 6 and $\rho(\tau)$ being given by eq 7. Figure 5c shows the best fit at 273 K. It improves largely the best fit in the single-time approximation (Figure 5a,b). The breadth of the distribution covers a range of about 2 decades.

For each temperature we fitted the ESR line shape by adjusting both the jump angle ϕ and the breadth of the distribution σ. Figure 6 shows the comparison between the experimental line shape at 289 K with the line shapes predicted by eqs 6 and 7 with $\sigma = 0.94$ and different jump angles ϕ. The best fit in the single-time approximation ($\sigma = 0$, $\phi = 30°$) is also shown for comparison. Once again, it is apparent that the use of a τ distribution improves the agreement between the theory and the experiment. We also note that there is an improvement if the jump angle ϕ is in the range 50°−80°. This optimal ϕ range was always found for $T < 360$ K where ESR may discriminate between different rotational models.

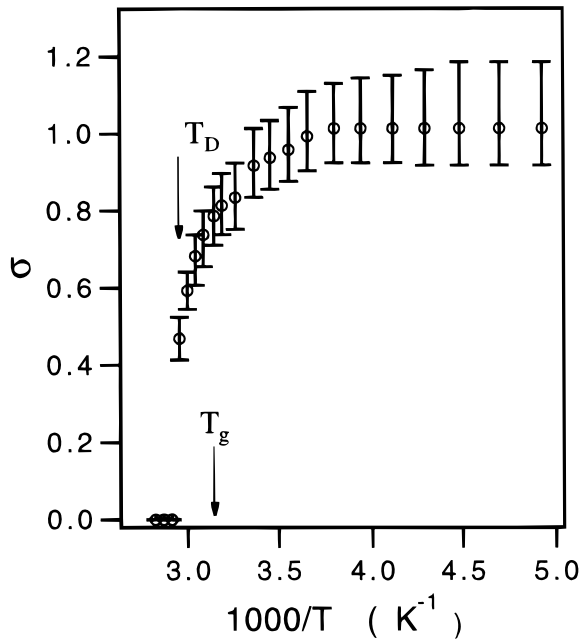

Figure 7. Temperature dependence of the width of the log-Gauss distribution $\rho(\tau)$. $\rho(\tau)$ vanishes at T_D.

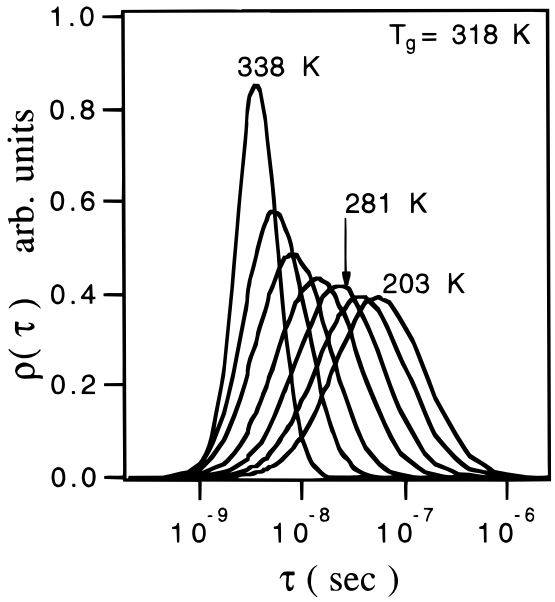

Figure 8. Representative plots of the log-Gauss distribution of the rotational correlation time $\rho(\tau)$.

B. Breadth of the Correlation Time Distribution $\rho(\tau)$. To characterize the rotational mechanism of the tracer in the rubbery and the glassy phase of PVAc, we studied the temperature dependence of the breadth of $\rho(\tau)$ (eq 7). Figure 7 shows the temperature dependence of the width σ. In the glassy region σ is approximately constant while in the rubbery state it drops steeply due to the narrowing of the distribution. $T_D = 338$ K $= T_g +$ 20 K is the temperature above which $\sigma = 0$ within the experimental errors. Representative plots of $\rho(\tau)$ are drawn in Figure 8. The plot shows that the distribution broadens at lower and lower temperatures, but well below T_g, it shifts to longer times without any change in the width. The finding agrees with recent studies of

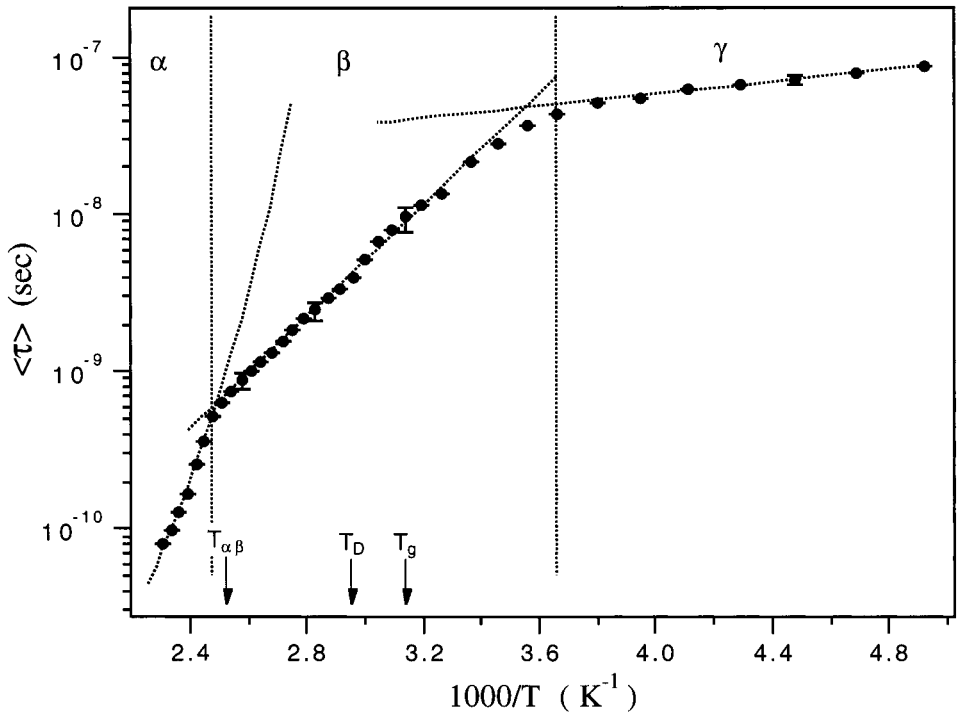

Figure 9. Arrhenius plot of $\langle\tau\rangle$. The superimposed dotted lines are VF with $\tau_0 = 7.8 \times 10^{-15}$ s, $B = 650$ K, $T_\infty = 265$ K (α region); Arrhenius laws with $\tau_1 = 2.21 \times 10^{-14}$ s, $\Delta E = 35$ kJ/mol (β region) and $\tau_1 = 9.5 \times 10^{-7}$ s, $\Delta E = 3.7$ kJ/mol (γ region). $T_{\alpha\beta}$ is the temperature where the α and β dielectric relaxations bifurcate. T_D is the temperature where the log-Gauss distribution vanishes (see Figure 7).

the rotational motion of probe molecules in polyisobutyl methacrylate carried out by second harmonic generation spectroscopy.[33]

Previous dielectric studies of PVAc fitted the distribution of relaxation times by a log-Gauss distribution[32] with a width σ_{diel}. A comparison between σ and σ_{diel} shows that $\sigma_{diel}/\sigma \approx 1.5$. The finding agrees well with the remark that the dielectric relaxations times $\langle\tau\rangle_\alpha$ and $\langle\tau\rangle_\beta$ are found 2 orders of magnitude longer than $\langle\tau\rangle$. The faster $\langle\tau\rangle$ and the smaller σ lends to the conclusion that the heterogeneous character of the tracer reorientation is partially averaged, probably due to the small size of the tracer which is well accommodated in the available free volume. Notably, the temperature dependence of the σ parameter of the present study and ref 32 evidences the breakdown of the time−temperature superposition principle in rubbery PVAc.

It is worthwhile to point out that tracers dissolved in materials close to their glass transition do not always exhibit distributions of rotational correlation times. As an example, no distribution was evidenced by dissolving the tracer TEMPO, which is nearly identical to the present tracer, in glassy *o*-terphenyl.[30]

C. Temperature Dependence of the Average Rotational Correlation Time $\langle\tau\rangle$. According to eq 7, the average rotational correlation time $\langle\tau\rangle$ takes the form

$$\langle\tau\rangle = \int \tau\rho(\tau)\, \mathrm{d}\ln\tau = \tau^* \exp\left[\frac{\sigma^2}{2}\right] \tag{8}$$

The parameters σ and τ^* of $\rho(\tau)$ are drawn by the fit of the ESR line shape. In Figure 9 the temperature dependence of $\langle\tau\rangle$ is shown. Three regions may be conveniently defined.

In region α ($T > 403$ K) the temperature dependence of $\langle\tau\rangle$ is well fitted by the Vogel−Fulcher law (VF):

$$\log\frac{\langle\tau\rangle}{\tau_0} = \frac{B}{T - T_\infty} \tag{9}$$

with $\tau_0 = (7.8 \pm 0.8) \times 10^{-15}$ s, $B = 650 \pm 60$ K, and $T_\infty = 265 \pm 18$ K. The B and T_∞ parameters compare nicely with the ones ($B = 660 \pm 50$ K, $T_\infty = 266 \pm 3.5$ K) drawn by the dielectric α relaxation.[34] The finding points to a coupling between the reorientation of the tracer and the structural relaxation of the polymer. It is worthwhile that the VF analysis of the α relaxation in PVAc by calorimetric, dielectric, and mechanical techniques led to B and T_∞ parameters being close to each other, whereas the τ_0 prefactors were found to be distributed over about 4 orders of magnitude.[34] This suggested a scaling property of the α relaxation of different physical quantities. According to the above result, the scaling extends also to the reorientation process of tracers being dissolved in the polymeric host.

The ratio $\langle\tau\rangle_\alpha/\langle\tau\rangle$ is about 300. We interpret this as mainly due to the different length scales that are involved. The length scale of the α relaxation may be estimated in the framewok of the Rouse model which predicts that modes with relaxation time τ extends over regions as wide as Δx where[35]

$$\Delta x = \left(\frac{3\pi^2 b^2 KT}{\zeta}\tau\right)^{1/4} \tag{10}$$

b and ζ are the length and the friction coefficient of the segment, respectively. K and T are the Boltzmann constant and the temperature, respectively. Being $\tau_\alpha \approx 10^{-7}$ s at 400 K yields[36] $\Delta x \approx 1$ nm, in good agreement with recent NMR studies in PVAc on dynamic heterogeneities[24] and mechanical properties[37] which detect length scales $\xi = 3 \pm 1$ nm. According to these studies, the α relaxation involves regions with volumes $\xi^3 \approx 27$ nm^3 to be compared with the tracer volume 0.18 nm^3.

Assuming that time and volume scale as $\tau \propto V^z$ yields $z = 1.14$ if $\xi = 3$ nm. Interestingly, hydrodynamics predicts $z = 1$ and Rouse model (see eq 10) $z = {}^4/_3$.[35,36] However, both predictions must be considered cautiously for time scales shorter than the one of α relaxation.[35,36]

In region β (403 K > T > 273 K), the temperature dependence of $\langle\tau\rangle$ is activated, i.e., $\langle\tau\rangle = \tau_1 \exp(\Delta E/KT)$, with $\Delta E = 35 \pm 6$ kJ/mol and apparent attempt time $\tau_1 = (2.21 \pm 0.7) \times 10^{-14}$ s. The ΔE value compares quite well with the activation energy of the β dielectric relaxation $\Delta E_\beta = 39 \pm 5$ kJ/mol.[38−41] This finding occurs very close to the temperature where the α and β processes bifurcate $T_{\alpha-\beta} \approx 395$ K $= T_g + 77$ K.[27,42] This is remarkable since it is well-known that dielectric relaxation does not investigate conveniently the α−β bifurcation region where the α and β peaks merge in a single broad structure. It is tempting to note that $T_{\alpha-\beta}$ is quite close to the crossover between the α and β regions of the relaxation map of the ^{15}N-DTEMPOL tracer (Figure 9). To conclude the discussion of the β region, we note that the ratio $\langle\tau\rangle_\beta/\langle\tau\rangle$ is about 160; i.e., it is larger than one-half of $\langle\tau\rangle_\alpha/\langle\tau\rangle$. It suggests that the β relaxation has not so local character as it could be expected. Ishida et al. reached the conclusion that the β relaxation arises from motions of the side groups which lead to, or are accompanied by, local distortions of the main chain.[27,44]

In region γ (T < 273 K) the temperature dependence is well described by the Arrhenius law with the activation energy 3.7 ± 0.6 kJ/mol and attempt time $\tau_1 = (9.5 \pm 1) \times 10^{-7}$ s. This value compares well with the activation energy of the γ relaxation $\Delta E_\gamma = 4.1 \pm 0.7$.[27,42,43] The ratio $\langle\tau\rangle_\gamma/\langle\tau\rangle$ is about 2.7. It suggests that the reorientation of TEMPOL relaxes due to molecular units of comparable size. The γ dielectric relaxation was ascribed to the methyl group located in the side chain.[45] Very recently, Colmenero and co-workers found by inelastic neutron scattering that the activation energy of the methyl group rotation of PVAc is 3.74 ± 0.27 kJ/mol, in nice agreement with our value, but the attempt time is in the picosecond region, i.e., 6 orders of magnitude faster than γ relaxation.[46] This lends to the conclusion that the molecular interpretation of the γ relaxation in PVAc is still an open matter.[27,39]

The above discussion points to the unifying conclusion that the tracer is well coupled to the relaxation mechanisms driving the dielectric response of PVAc. Being the latter mainly due to the polar groups of the side chains, one concludes the tracer is located preferentially close to the latter.

Other ESR investigations dealing with the rotational correlation times of paramagnetic tracers in PVAc are reported. Li and Gelerinter presented a study of the rotational motion of TEMPOL in PVAc.[45] Differently from the present study, TEMPOL was neither deuterated nor ^{15}N-enriched. The analysis of the ESR line shape does not account for the τ distribution and is based on the diffusion model. This simplified model leads to rotational correlation times that agree with ours in the α and γ regions. However, as widely discussed in section IIIA, the diffusion model fits poorly the ESR line shape (see also Figure 3 of ref 45). In fact, discrepancies are found in the β region (403 K > T > 273 K) where the τ distribution vanishes in a narrow temperature range (see Figure 7), and expectedly, the rotational model must be refined. The rotational diffusion of the tracer DBOZ, which is quite similar to TEMPOL, in PVAc was studied by Miles et al.[42] The analysis was carried out using the same guidelines as ref 45. The correlation times are found to be 1 order of magnitude longer than ours and the ones of ref 45. If the data are suitably shifted, a broad agreement with our results is found in the α and γ regions, whereas the β region is poorly characterized.

We would like to end the section by noting that the reorientation of the tracer in the α region cannot be interpreted in terms of the usual Debye−Stokes−Einstein equation (DSE)

$$\langle\tau\rangle = \frac{V\eta}{kT} \tag{11}$$

where V and η are the tracer volume and the shear viscosity, respectively. In fact, $\eta(410\text{ K}) \cong 1.8 \times 10^5$ P[47] (the scaling $\eta \propto \text{MW}^{3.4}$ was used to account for the different MW's), and eq 11 yields $\langle\tau\rangle \cong 7.8 \times 10^{-4}$ s, i.e., about 5 orders of magnitude larger than the experimental values. This huge discrepancy clearly proves that the reorientation of the tracer is not driven by the viscous flow of the polymer.

IV. Conclusions

We studied by ESR the rotational motion of a paramagnetic probe dissolved in PVAc. The use of a fully deuterated probe with nuclear spin $I = {}^1/_2$ simplified and sharpened the pattern of the ESR line shape. The improved resolution allowed a thorough characterization of the tracer reorientation via the numerical simulation of the ESR line shape. In particular, it was found that the reorientation of the tracer occurs via jumps of about 50° with a heterogeneous distribution of correlation times. The breadths of the distributions of the rotational correlation time and the dielectric relaxation time are found to be close ($\sigma_{\text{diel}}/\sigma \approx 1.5$).

A unifying interpretation of the results is given by pointing out that the average correlation time $\langle\tau\rangle$ tracks the dielectric relaxation of PVAc. Being the dielectric relaxation of PVAc mainly due to the polar groups located in the side chains, the tracer is then located preferentially close to the latter. On cooling, $\langle\tau\rangle$ tracks the α relaxation down to about the α−β bifurcation temperature and then the β relaxation down to about the glass transition. The characterization of the α−β bifurcation region where dielectric relaxation studies got into difficulties is one of the main results of the present work. The ratio $\langle\tau\rangle_\alpha/\langle\tau\rangle = C_\alpha = 300$ has been interpreted in terms of the different length scales of the α relaxation and the tracer size. The approximate equality $C_\alpha \approx C_\beta$ suggests that the β relaxation has not a complete local character in agreement with other studies.[27] $C_\gamma \approx 3$ is ascribed to the comparable size of the molecular unit involved in the γ relaxation and the tracer.

We expect that dielectric and mechanical relaxation may be tracked also in other polymers by using stiff tracers of limited size. Additional work is needed to gain more insight into the role of the tracer to enhance the coupling with the relaxation modes.

Acknowledgment. The authors thank Prof. H. W. Spiess for the kind donation of the sample. Discussions with Dr. Dino Ferri, ENICHEM Research Center, Mantova, are gratefully acknowledged.

References and Notes

(1) Dhinojwala, A.; Wong, G. K.; Torkelson, J. M. *Macromolecules* **1992**, *25*, 7395.
(2) Dhinojwala, A.; Wong, G. K.; Torkelson, J. M. *Macromolecules* **1993**, *26*, 5943.
(3) Dhinojwala, A.; Wong, G. K.; Torkelson, J. M. *J. Chem. Phys.* **1994**, *100*, 6046.
(4) Dhinojwala, A.; Hooker, J. C.; Torkelson, J. M. *J. Non-Cryst. Solids* **1994**, *172−174*, 286.
(5) Hooker, J. C.; Torkelson, J. M. *Macromolecules* **1995**, *28*, 7683.
(6) Blackburn, F. R.; Cicerone, M. T.; Hietpas, G.; Wagner, P. A.; Ediger, M. D. *J. Non-Cryst. Solids* **1994**, *172−174*, 256.
(7) Ye, J. Y.; Hattori, T.; Nakatsuka, H.; Maruyama, Y.; Ishikawa, M. *Phys. Rev. B* **1997**, *56*, 5286.
(8) Andreozzi, L.; Di Schino, A.; Giordano, M.; Leporini, D. *Europhys. Lett.* **1997**, *38*, 669.
(9) Bagliesi, M. G.; Cianflone, F.; Leporini, D. *Mater. Res. Soc. Symp. Proc.* **1997**, *455*, 157.
(10) Andreozzi, L.; Giordano, M.; Leporini, D. *J. Non-Cryst. Solids* **1998**, *235−237*, 219.
(11) Andreozzi, L.; Di Schino, A.; Giordano, M.; Leporini, D. *Philos. Mag.* **1998**, *77*, 547.
(12) Andreozzi, L.; Chiellini, E.; Giordano, M.; Leporini, D. *Mol. Cryst. Liq. Cryst.* **1995**, *266*, 73.
(13) Andreozzi, L.; Cianflone, F.; Galli, G.; Giordano, M.; Leporini, D. *Mol. Cryst. Liq. Cryst.* **1996**, *290*, 1.
(14) Muus, L. T., Atkins, P. W., Eds. *Electron Spin Relaxation in Liquids*; Plenum: New York, 1972.
(15) Berliner, L. J., Ed. *Spin Labeling Theory and Applications*; Academic Press: New York, 1976.
(16) Cameron, G. G. In *Comprehensive Polymer Science*; Booth, C., Price, C., Eds.; Pergamon: Oxford, 1989.
(17) Rånby, B.; Rabek, J. F. *ESR Spettroscopy in Polymer Research*; Springer: Berlin, 1977.
(18) Kashiwabara, H.; Shimada, S.; Hori, Y.; Sakaguchi, M. *Adv. Polym. Sci.* **1987**, *82*, 141.
(19) Andreozzi, L.; Giordano, M.; Leporini, D. In *Structure and Transport Proprieties in Organized Polymeric Materials*; Chiellini, E., Giordano, M., Leporini, D., Eds.; World Scientific: Singapore, 1998.
(20) Hubrich, M.; Maresch, G. G.; Spiess, H. W. *J. Magn. Reson.* **1995**, *A113*, 177.
(21) Volkmer, T.; Wiesner, U.; Brombacher, L.; Spiess, H. W. *Macromol. Chem. Phys.* **1996**, *197*, 1121.
(22) Saalmueller, J. W.; Long, H. W.; Maresch, G. G.; Spiess, H. W. *J. Magn. Reson.* **1995**, *117*, 193.
(23) Saalmueller, J. W.; Long, H. W.; Volkmer, T.; Wiesner, U.; Maresch, G. G.; Spiess, H. W. *J. Polym. Sci., Part B: Polym. Phys.* **1996**, *34*, 1093.
(24) Tracht, U.; Wilhelm, M.; Heuer, A.; Feng, H.; Schmidt-Rohr, K.; Spiess, H. W. *Phys. Rev. Lett.* **1998**, *81*, 2727.
(25) Giordano, M.; Grigolini, P.; Leporini, D.; Marin, P. *Adv. Chem. Phys.* **1985**, *62*, 321.
(26) Andreozzi, L.; Giordano, M.; Leporini, D. *Appl. Magn. Reson.* **1992**, *4*, 279.
(27) McCrum, N. G.; Read, B. E.; Williams, G. *Anelastic and Dielectric Effects in Polymeric* Solids; Wiley: New York, 1967.
(28) Victor, J. G.; Torkelson, J. M. *Macromolecules* **1987**, *20*, 2241.
(29) Ivanov, E. N. *Sov. Phys. JETP* **1964**, *18*, 1041.
(30) Andreozzi, L.; Cianflone, F.; Donati, C.; Leporini, D. *J. Phys.: Conden. Matter* **1996**, *8*, 3795.
(31) Montroll, E. W.; Bendler, J. T. *J. Stat. Phys.* **1984**, *34*, 129.
(32) Nozaki, R.; Mashimo, S. *J. Chem. Phys.* **1987**, *87*, 2271.
(33) Hall, D. B.; Dhinojwala, A.; Torkelson, J. M. *Phys. Rev. Lett.* **1997**, *79*, 103.
(34) Beiner, M.; Korus, J.; Lockwenz, H.; Schroter, K.; Donth, E. *Macromolecules* **1996**, *29*, 5183.
(35) Doi, M.; Edwards, S. F. *The Theory of Polymer Dynamics*; Clarendon: Oxford, 1986.
(36) Ferry, J. D. *Viscoelastic Properties of Polymers*; Wiley: New York, 1980.
(37) Donth, E.; Beiner, M.; Reissig, S.; Korus, J.; Garwe, F.; Vieweg, S.; Kahle, S.; Hampel, E.; Schroter, K. *Macromolecules* **1996**, *29*, 6589.
(38) Starkweather, H. W. *Macromolecules* **1988**, *21*, 1798.
(39) Hoch, M. J. R.; Bovey, F. A.; Davis, D. D.; Douglass, D. C.; Falcone, D. R.; McCall, D. W.; Slichter, W. P. *Macromolecules* **1971**, *4*, 713.
(40) Ishida, Y.; Matsuo, M.; Yamafuji, K. *Kolloid Z.* **1962**, *180*, 108.
(41) Hikichi, K.; Furuichi, J. *Rep. Prog. Polym. Phys.* **1961**, *4*, 69.
(42) Miles, I.; Cameron, G. A.; Bullock, T. *Polymer* **1986**, *27*, 190.
(43) Thurn, H.; Wolf, K. *Kolloid Z.* **1956**, *148*, d6.
(44) Yamafuji, K.; Ishida, Y. *Kolloid Z.* **1962**, *183*, 15.
(45) Li, J.; Gelerinter, E. *Polymer* **1992**, *33*, 963.
(46) Colmenero, J.; Mukhopadhyay, R.; Alegria, A.; Frick, B. *Phys. Rev. Lett.* **1998**, *80*, 2350.
(47) Plazek, D. J. *Polym. J.* **1980**, *12*, 43.

MA981178X